

000 001 002 003 004 005 006 007 008 009 010 011 012 013 014 015 016 017 018 019 020 021 022 023 024 025 026 027 028 029 030 031 032 033 034 035 036 037 038 039 040 041 042 043 044 045 046 047 048 049 050 051 052 053 AN ONTOLOGY ENRICHMENT FRAMEWORK USING RETRIEVAL-AUGMENTED LARGE LANGUAGE MOD- ELS

Anonymous authors

Paper under double-blind review

ABSTRACT

Ontology enrichment, understood as the process of extending and refining existing ontologies with new concepts, relations, and instances, has become a critical task for building robust and up-to-date knowledge bases. The exponential growth of scientific publications, datasets, and multimodal resources makes manual enrichment highly impractical, creating the need for automated or semi-automated approaches. In this work, we propose a framework that leverages multimodal large language models and retrieval-augmented generation to support ontology enrichment. Our method systematically extracts semantic knowledge units, aligns them with existing ontological structures, and generates interlinked triples, thereby enhancing both the coverage and the expressivity of the ontology. This framework addresses the knowledge acquisition bottleneck by enabling scalable integration of heterogeneous resources and fostering cross-domain semantic interoperability. To illustrate its effectiveness, we apply the framework to the domain of 4D printing, a rapidly evolving field at the intersection of materials science, manufacturing, and design. By incorporating knowledge about materials, properties, stimuli interactions, process parameters, and design strategies, the framework enriches a domain-specific ontology and supports innovation in the development of programmable and multifunctional structures. The proposed framework follows a four-stage pipeline that combines multimodal retrieval of relevant text and figures from scientific literature with the ingestion of structured datasets and existing knowledge graphs, uses a fine-tuned multimodal LLM to extract ontology-aligned triplets, applies multi-criteria validation based on semantic relevance and consistency, and finally performs ontology population through symbolic reasoning.

1 INTRODUCTION

In the era of artificial intelligence (AI) and data-driven technologies, the ability to structure and interpret knowledge has become a cornerstone of intelligent systems. While vast amounts of data are continuously generated, their utility depends on transforming raw information into machine-readable semantic representations. Ontologies have emerged as a key solution to this challenge, providing a formal and explicit specification of a shared conceptualization of a domain (Gruber, 1993). They allow the definition of concepts, properties, and semantic relations, which enables reasoning, knowledge integration, and inference beyond the explicitly available information (Guarino et al., 2009). Ontologies play a central role in the development of the Semantic Web, where they serve as the backbone for annotating and linking web resources with machine-interpretable semantics (Shadbolt et al., 2006). Instead of being limited to unstructured or human-centered information, the Semantic Web envisions a knowledge-rich environment where data can be shared, reused, and reasoned upon across heterogeneous systems. This has led to a significant research focus on domain- and task-specific ontologies, which are increasingly applied in diverse fields such as biomedicine (Bodenreider, 2004), materials science (Ghedini et al., 2017), and manufacturing (Chungoora et al., 2013). Similarly, the HERMES (spatiotemporal semantics and logical knowledge description of me-
chanical objEcts in the era of 4D pRinting and programmable Matter for nExt-generation of CAD systemS) domain ontology has been established to capture 4D printing knowledge at the part design level (Dimassi et al., 2021).

Despite their structured nature, traditional ontologies are limited in dynamically adapting to evolving knowledge and in processing unstructured textual data and natural language inputs. These shortcomings highlight the need for enhanced integration between ontological systems and AI, particularly through natural language processing (NLP) and machine learning (ML) techniques (Li, 2018). Scaling LLMs has led to emergent reasoning capabilities, including in-context learning (ICL) (Peng et al., 2023), chain-of-thought (CoT) (Wei et al., 2022), and retrieval-augmented generation (RAG) (Gao et al., 2023). These advances mitigate some limitations of conventional AI models by enabling real-time knowledge retrieval and contextual inference. Additionally, the recent development of multimodal LLMs (MLLMs) has further expanded AI's ability to integrate textual, visual, and symbolic information (Yin et al., 2024). These models are particularly relevant for domains like 4D printing, where information must be captured across modalities to support design synthesis.

Through these advancements, LLMs remain fundamentally limited in interpretability and domain specificity. Their probabilistic nature can lead to hallucinations and unreliable outputs, particularly in highly specialized fields like 4D printing. Ontologies, by contrast, offer structured and interpretable knowledge representation but lack adaptability. The fusion of both technologies presents a promising approach to overcoming these challenges, especially in the enrichment of ontological data structures, termed as ontology learning. As manual annotation is labor-intensive and not scalable for large datasets or rapidly changing domains, semi-automatic methods, such as Phrase2Onto (Pour et al., 2023), have been developed by suggesting new concepts through phrase-based topic modeling; however, they still rely heavily on user input for validation, introducing potential subjectivity and inconsistency. Fully automated approaches using NLP and ML expedite the ontology extension process but are dependent on the quality of training data. These may introduce biases or errors if the data or models are not well-aligned with domain specifics. Advanced systems like online clustering with LLM agents (Wu et al., 2024) provide innovative ways to integrate new knowledge without extensive annotated datasets. However, they struggle with maintaining consistency and effectively integrating diverse information streams, posing challenges in ensuring the accuracy and relevance of ontology extensions.

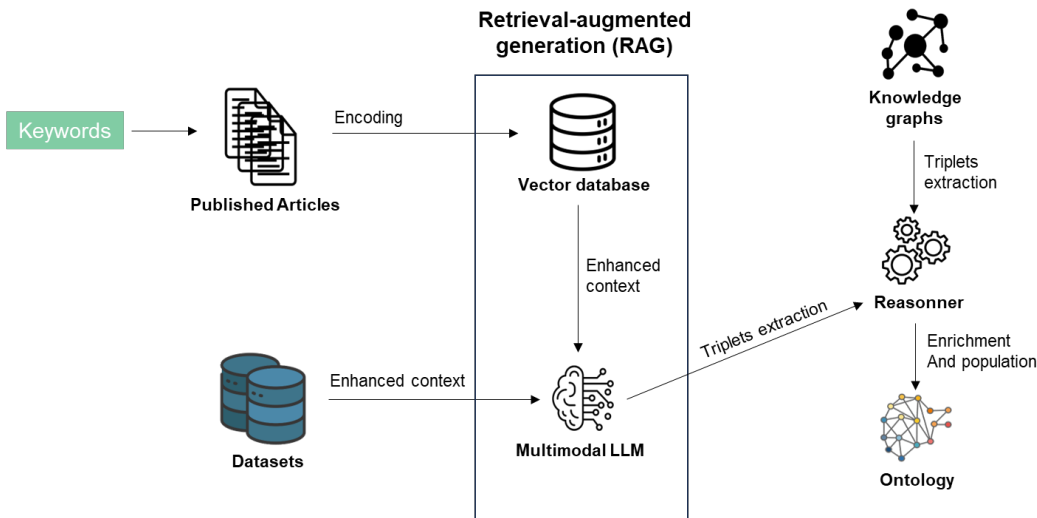
The emergence of 4D printing – a technology combining smart materials and additive manufacturing (AM) – has opened new frontiers in fields requiring adaptive, deployable, or transformative structures (Demoly & André, 2022a;b). This paradigm enables objects to self-transform in response to external stimuli such as heat, light, moisture, solvent, or magnetic/electric fields (Tibbits, 2013; Ge et al., 2013). The scientific landscape of 4D printing is both rapidly evolving and inherently multidisciplinary, encompassing fields such as materials science, chemistry, mechanical engineering, process engineering, and biomimicry (Demoly et al., 2021). Since its inception in 2013, the field has experienced exponential growth, with more than 3,500 publications and an estimated annual growth rate of approximately 40%, according to the Web of Science database (Demoly & André, 2021; Demoly & André, 2021; 2024). Key challenges in advancing 4D printing include improving the printability of smart materials, enhancing their mechanical and actuation performance, promoting safe and sustainable deployment, and ensuring reliability under cyclic stimuli and real-world conditions (Demoly et al., 2021). These challenges can be considered as interdependent, especially when designing and developing practical 4D-printed systems, where trade-offs between material properties, process parameters, and functional requirements must be carefully balanced (Demoly et al., 2021). To support collective and coherent progress, it becomes vital to establish a comprehensive and dynamic knowledge and data infrastructure capable of integrating both historical findings and emerging research. Such an infrastructure is crucial for consolidating the existing body of knowledge and effectively guiding future developments.

The proposed retrieval-augmented MLLMs framework aims to integrate ontology-based reasoning with the generative and retrieval capabilities of MLLMs to support knowledge discovery across diverse domains. By embedding ontological structures within LLM architectures, the framework enhances knowledge extraction, semantic reasoning, and adaptive learning from both structured and unstructured data sources, ranging from scientific literature and datasets. This active ontology enrichment approach ensures real-time alignment with emerging research and technological advancements. To demonstrate its applicability, we apply this framework to the domain of 4D printing, where it enables the integration of cross-disciplinary insights related to smart materials, processes, and programmable structures.

108

2 ONTOLOGY ENRICHMENT FRAMEWORK

109
 110 Ontology enrichment enables the enhancement of an existing preliminary ontology by automatically
 111 adding new concepts (also considered as knowledge), relationships, and individuals (meaning
 112 information or data) to make it more comprehensive and practical for a specific domain or task. To
 113 ensure both the enrichment and population of the initial ontology, we employ an integrated frame-
 114 work combining information retrieval with advanced text generation capabilities (as illustrated in
 115 **Figure 1**).



134 Figure 1: Retrieval-augmented ontology construction pipeline (adapted from (Bougmez et al.,
 135 2025b)).
 136

137 Initially, we collected a curated corpus of published articles and domain-specific datasets using
 138 targeted keywords. Each published article is split into discrete text segments and extracted figures,
 139 while each dataset table is parsed into individual records. All text and image snippets are then
 140 encoded using a fine-tuned MLLM into dense vectors and stored in a high-throughput vector index.
 141 At inference time, the LLM issues similarity queries against this index to retrieve the top-k relevant
 142 passages or images, which it incorporates as “context windows” into its prompts. From the generated
 143 and context-aware outputs, a downstream triplet-extraction module identifies candidate [Subject-
 144 Predicate- Object] facts. These facts are merged with existing knowledge from knowledge graphs
 145 and passed to a symbolic reasoner, which enforces ontology schema constraints, checks for logical
 146 consistency, and removes duplicates. Resulted triplets are then translated into classes, properties, or
 147 instances, thereby populating and enriching the initial ontology in a continuous loop that keeps our
 148 knowledge base both up to date and semantically rigorous.
 149

150 2.1 ONTOLOGY ENRICHMENT FROM SCIENTIFIC LITERATURE

151 To enrich the ontology, the process begins with the identification and selection of key terms relevant
 152 to the domain of interest. Using the ResearchRabbit application tool (res, 2025), an AI-supported
 153 scholarly discovery platform, the pertinent intersections among these keywords serve as the basis
 154 for collecting a large body of published research.

155 Then, we split these published articles using tools like LLM Sherpa (Nlm-atics, 2024) for robust text
 156 extraction and semantic chunking, which divided each paper into coherent chunks based on struc-
 157 tural elements. This approach was designed to optimize both semantic completeness and compu-
 158 tational efficiency, ensuring that each segment retained meaningful contextual information. Chunk
 159 boundaries followed the natural discourse flow (e.g., paragraphs or logical sections) rather than fixed
 160 lengths, thereby preserving local coherence throughout the segmentation process. The Aspose tool
 161 (Aspose, 2024) was used for image extraction in order to isolate each figure into standalone image
 files. Each token was then embedded using BERT model and CLIP for images. This process con-

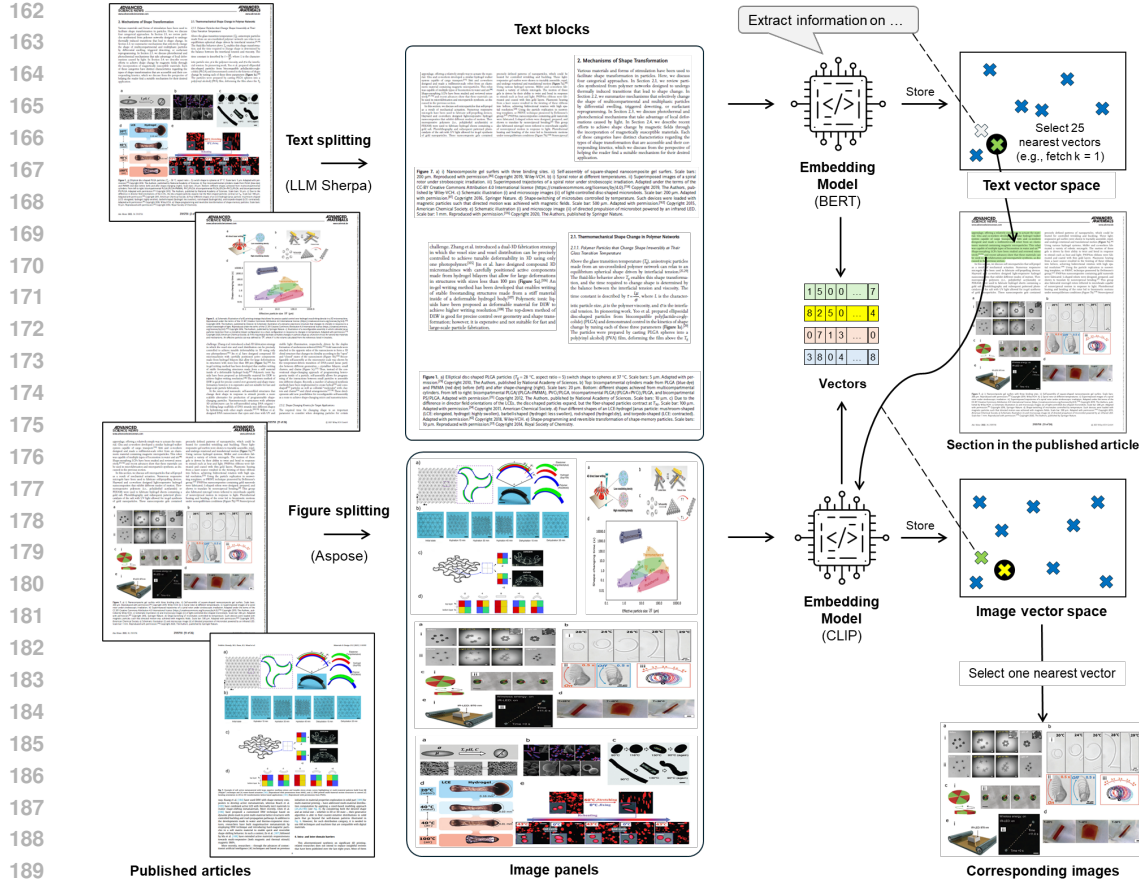


Figure 2: Pipeline for extracting textual sections and associated figures from scientific literature (adapted from (Bougzime et al., 2025b)).

verts the content into vector representations, allowing us to store them in a vector space, as shown in **Figure 2**.

Subsequently, detailed information concerning domain-specific entities, processes, and methodologies is systematically extracted from textual sources. Queries are encoded within a text vector space using BERT embeddings to identify the 25 nearest vectors. As illustrated in **Figure 2**, selecting one text vector highlights the section in green as the most relevant to the query. This section serves to identify and retrieve its corresponding relevant image through the CLIP embedding model and image vector space.

By pairing each textual section with its corresponding image, we enriched the LLaVA (Large Language-and-Vision Assistant) MLLM’s input context (Parthasarathy et al., 2024; Kim et al., 2023; Jeong, 2024). This RAG process combines information retrieval with text generation, so that it helps to address challenges such as hallucination, outdated knowledge, and opaque reasoning in language models. By incorporating data from external databases, RAG ensures more accurate and credible output, particularly in knowledge-intensive tasks. This integration facilitates ongoing updates and the inclusion of specialized information, therefore making RAG a dynamic solution that combines intrinsic model knowledge with extensive external data.

Initially, we employed a few-shot learning strategy (Brown et al., 2020; Hoffmann et al., 2022; Yang et al., 2022); however, this approach proved inefficient due to the long context windows required, leading to high computational and memory costs as well as imprecise extractions. To improve efficiency and robustness, we fine-tuned the LLaVA model specifically for ontology-aligned triplet extraction (Ghanem & Cruz, 2024; Liu et al., 2022; Zhang et al., 2024), using Low-Rank Adaptation

(LoRA) (?) as a parameter-efficient fine-tuning (PEFT) method (Lialin et al., 2023). LoRA significantly reduces the computational footprint of fine-tuning, allowing us to specialize the model for our domain without full model retraining. This process involved embedding domain-specific knowledge within the LLaVA model, thus configuring the output format appropriately and ensuring consistent performance without the need for additional tokens. During fine-tuning, domain-specific knowledge was embedded into LLaVA so that the model could reliably distinguish ontology classes, data properties, object properties, and instances, while also preserving hierarchical constraints compliant with OWL formalism (Val-Calvo et al., 2025; Doumanas et al., 2025). This approach aims to refine a multimodal large language model into a tool capable of identifying ontology-relevant triplets within a specific domain. Additional implementation details and hyperparameters are provided in Appendix C.

To enable fine-tuning, a synthetic dataset is generated using a LLM. Relevant textual sections are extracted from a corpus of scientific articles, and the CLIP model is employed to retrieve the most semantically aligned image for each section. These image–text pairs are transformed into prompts, which, through a one-shot learning approach with carefully designed instructions, guide a large language model (e.g., ChatGPT-4) to generate both detailed textual descriptions and structured triplets in the form of [Subject–Predicate–Object]. The resulting dataset follows a standardized format: [prompt (combining the section and the image), triplets], and consisted of 230 ground truth examples validated by a 4D printing expert, because direct prompting of frontier models frequently produces hallucinated or ontology-inconsistent triplets and therefore still requires extensive expert validation.

During inference, a single multimodal prompt was constructed for each target section. This prompt included: (i) the raw section text, (ii) the associated figure or schematic, and (iii) a directive stating “Extract all domain-relevant triplets”. This prompt was then processed by our MLLM, which jointly attended to textual tokens and image patches to generate a set of [subject, predicate, object] assertions. For figures, the model first employed an optical character recognition (OCR) module to detect and encode text regions, and to extract key graphical elements (i.e., shapes, connectors, symbols) as visual tokens. These visual tokens interacted with text embeddings via cross-attention within the multimodal transformer. The text embeddings had been refined through our fine-tuning procedure, therefore allowing for better alignment with domain-specific semantics. This cross-modal mechanism enabled the model to infer high-level semantic relations that are not explicitly stated in the input but emerge from a combination of spatial configurations, textual cues, and prior knowledge encoded in the pretrained weights. For example, in a section from Peng et al.’s paper (Peng et al., 2022), illustrated in Figure 3A, describing liquid crystal elastomer (LCE) preparation, the spatial proximity and labels of “EDDET” and “PETA” enabled the model to infer an `isCrosslinkedWith` relation, which leverages both the visual structure and domain-specific patterns learned during pretraining. As shown in Figure 3B, relations grounded purely in the text (e.g., LCE_{link} `isComposedOf` TEA) are rendered in blue, whereas those inferred from the figure’s spatial layout and graphical elements (e.g., RM257 `isCombinedWith` RM82) appear in red. This example illustrates why multimodality is essential in our setting: many scientifically relevant relations are encoded exclusively within figures or schematics rather than in the surrounding text. This integrated multimodal approach thus ensures a reliable extraction of triplets from both explicit textual descriptions and implicit visual patterns.

2.2 ONTOLOGY ENRICHMENT FROM EXISTING DATASETS

To enhance the ontology, specific datasets that align with the domain’s requirements are incorporated. The selection process considers both the relevance of the datasets and their compatibility with format constraints. Integration into the ontology follows a systematic methodology involving detailed data preparation and mapping. Each dataset is decomposed into its constituent columns, which are described and cataloged, with examples provided for clarity. To categorize each attribute within the ontology, a one-shot learning approach (Li et al., 2023; Ucar et al., 2020) supported by a large language model (Jiang et al., 2023) is applied. Each cell in every row is instantiated as an individual of its corresponding ontology class, as illustrated in Figure 4, and resource description framework (RDF) object properties are extracted to link these instances. For example, in the Hy-

270 A
271
272 <system>
273 Identify the most relevant triplets within the field of additive manufacturing
or 4D Printing based on the given supplementary context and image
analysis.

<|user|>
Supplementary context:

RESEARCH ARTICLE

4D Printing of Free-standing Liquid Crystal Elastomers via Hybrid Additive Manufacturing

→ (Rw62.Rw257 / weight ratio = 75:25) were mixed with the diethol spacer EDEDT and the crosslinker PETA. The molar ratio was 1.16:1.0:18 for thiol:LC acrylate:crosslinker acrylate. The mixture was melted at 80 °C, and mixed with 0.6 wt% of PI 784, 2.5 wt% of BHT, and 0.6 wt% of TEA.

<|assistant

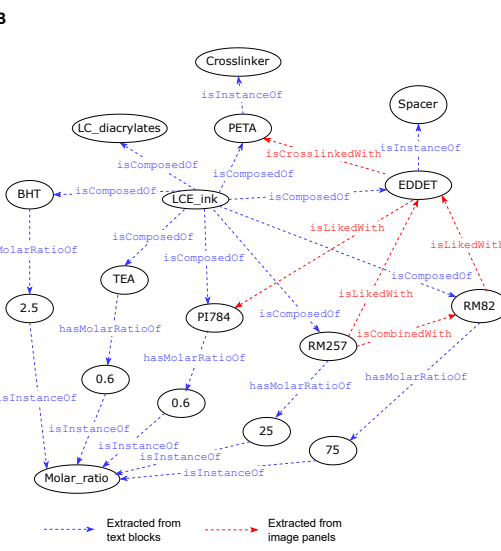


Figure 3: Example of the inference pipeline: (A) a section is selected from a published article in *Advanced Materials* Journal (Peng et al., 2022), its most relevant image was retrieved, and (B) a corresponding graph of triplets was produced.

drogel Design dataset (hyd, 2023; Richbourg et al., 2021; Richbourg & Peppas, 2023) we created instances for classes such as **Polymer**, **SwellingRatio**, and **ShearModulus_kPa**, and generate relations – e.g., **Polymer** linked via `hasShearModulus` to **ShearModulus_kPa**, **Polymer** linked via `hasSwellingRatio` to **SwellingRatio**, and **SwellingRatio** linked via `influencesShearModulus` to **ShearModulus_kPa**. This end-to-end pipeline yields a richly interconnected ontology graph that faithfully captures both the structural typology and the relational semantics of the original data.

2.3 ONTOLOGY ENRICHMENT FROM KNOWLEDGE GRAPH

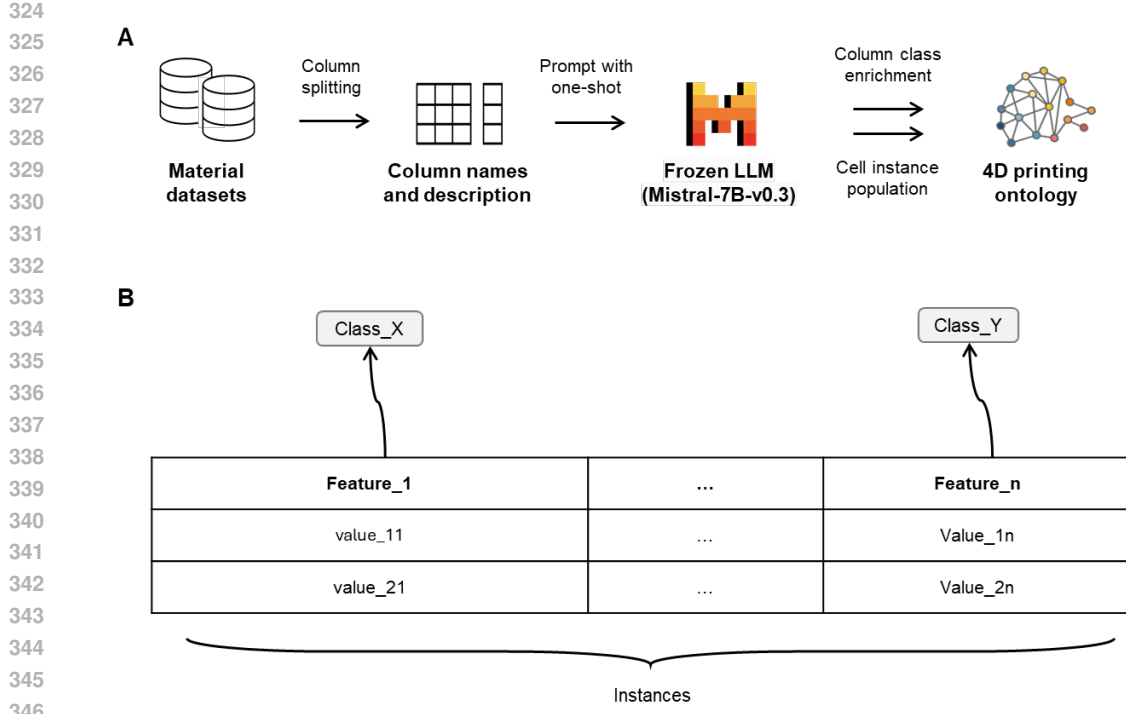
Furthermore, large-scale domain knowledge graphs can be leveraged to enrich ontologies with structured knowledge. Their integration typically relies on a systematic transformation pipeline that represents information in the standard [Subject, Relation, Object] format. To ensure semantic consistency and interoperability, relationship mapping strategies are applied to align the extracted relations with the target ontology.

2.4 PREPROCESSING AND CONSTRUCTION OF THE ONTOLOGY

The results produced by the framework are subjected to a rigorous cleaning process to ensure that only high-quality triplets are retained. In particular, the evaluation process considers the following aspects :

Domain relevance: Each triplet’s subject and object are transformed into contextualized embeddings using BERT and compared against embeddings derived from a curated list of domain-specific keywords. For each triplet element, the framework computes cosine similarity scores against all domain keywords and retains the maximum similarity value as the relevance indicator. The final domain relevance assessment combines both subject and object relevance scores in the overall evaluation function. This process ensures that the data is deeply aligned with the target field.

Semantic coherence: The framework implements a comprehensive evaluation strategy to assess semantic meaningfulness. It computes direct BERT-based cosine similarity between subject and object embeddings to measure their semantic relatedness. The final coherence score integrates both the relation validity and subject-object similarity components. Additionally, predicate coherence is evaluated through template-based assessment, where the framework compares BERT embeddings



348 Figure 4: (A) Overview of the dataset pipeline, and (B) illustration of identified classes and instances
349 related to a dataset representation (adapted from (Bougzime et al., 2025b)).

355 of complete triplet phrases against baseline phrases and relationship templates to ensure predicate
356 appropriateness within the semantic context.

357 **Structural validity:** The framework checks the syntactic correctness of each triplet by verifying
358 that all elements (subject, predicate, and object) are present, of sufficient length, and follow expected
359 formatting standards. This validation ensures data reliability for downstream applications.

360 **Redundancy elimination:** Duplicate or highly similar triplets are identified through a two-stage
361 process. First, exact duplicates are removed through string matching of subject-predicate-object
362 combinations. Second, semantic duplicates are detected by computing BERT-based cosine similarity
363 between triplet embeddings, where triplets exceeding a similarity threshold are flagged as redundant.
364 This ensures that the final dataset is concise and free from both literal and semantic redundancy.

366 Together, these validation steps contribute to a robust and high-fidelity cleaning process that pre-
367 pares the data for subsequent ontology construction and analysis. In addition to these quality control
368 measures, the ontology construction phase integrated several advanced techniques to further enhance
369 the ontology. First, entity names are normalized and cleaned to create valid uniform resource identi-
370 fier fragments, thereby ensuring semantic consistency across the ontology. This preprocessing step
371 effectively mitigates errors arising from formatting discrepancies or lexical variations. Furthermore,
372 the framework incorporates a BERT-based similarity analysis that compares new class labels with
373 those already present in the ontology. This mechanism dynamically identifies semantically similar
374 classes and, when a sufficient similarity threshold is met, establishes subclass relationships. In doing
375 so, the ontology consolidates redundant entities and organizes them hierarchically in a manner that
376 mirrors the underlying domain structure. Moreover, special attention has been given to maintaining
377 the homogeneity of the complete ontology by enforcing uniform naming conventions and consistent
semantic representations across all entities. This ensures that the entire knowledge base exhibits a
high degree of internal consistency, which is critical for efficient reasoning and data integration.

378 3 RESULTS: APPLYING THE FRAMEWORK TO 4D PRINTING ONTOLOGY

380
 381 The rapid advancements in 4D printing have introduced a need for a structured framework to manage
 382 and formalize the diverse knowledge involved in designing transformable systems. The HERMES
 383 ontology addresses this need by providing a semantic and logical foundation for representing the
 384 dynamic behavior of 4D-printed objects (Dimassi et al., 2021). Built upon the Basic Formal On-
 385 tology (Arp et al., 2015) and mereotopology theory (Smith, 1996), this ontology is centered on
 386 key 4D printing views, namely AM, material, transformation process, and design and engineering.
 387 Although structured around philosophical foundations and DL rules to ensure expressivity and rea-
 388 soning across abstraction levels, this ontology – like most existing material ontologies – suffers from
 389 limited capabilities for automated and large-scale learning through enrichment and population. This
 390 limitation is particularly critical in emerging and rapidly evolving research domains like 4D print-
 391 ing, where knowledge consolidation is essential to enhance technological readiness levels and reach
 392 practical applications.

392 To enrich the ontology, the process starts with the selection of key terms, ie., “Additive Manufac-
 393 turing”, “3D/4D Printing”, “Shape Memory Polymer”, “Shape Memory Alloy”, “Liquid Crystal
 394 Elastomer”, “Hydrogel”, “Active/Smart Material”, “Metamaterial”, and “Multi-Material Structure”.
 395 By identifying the pertinent intersections among these keywords, more than 1,810 relevant publica-
 396 tions were retrieved. These articles are then decomposed into textual sections and extracted figures,
 397 which are encoded into dense vectors and indexed within a high-performance retrieval store. In
 398 parallel, material datasets collected from eight specialized databases (Jain et al., 2013b; Kuenneth
 399 & Ramprasad, 2022; hyd, 2023; Crews et al., 2012; University of Chicago, 2023; Jain et al., 2013a;
 400 Takahashi et al., 2024; NASA, 2025) undergo a column-centric processing pipeline: column names
 401 and descriptions are parsed and mapped to ontology classes using a one-shot prompting technique
 402 with an LLM, thereby instantiating each row as an instance of its corresponding class and uncov-
 403 ering relationships among the fields. At inference, the MLLM retrieves the most relevant text or
 404 image snippets and generates context-aware outputs, from which a dedicated extraction module de-
 405 rives candidate triples. These newly extracted triples, together with pre-existing entries from the
 406 MATKG knowledge graph (Venugopal & Olivetti, 2024), are then passed to a downstream symbolic
 407 reasoner. The reasoner performs rigorous validation—ensuring coherence, semantic consistency,
 408 structural integrity, and duplicate elimination—before constructing and enriching the HERMES on-
 409 tology. The quality of the extracted triplets is underpinned by a Graph BERTScore F1 (Saha et al.,
 410 2021) of 0.7, demonstrating high semantic fidelity (see Appendix A). This integrated multimodal
 411 approach thus ensures a reliable extraction of triplets from both explicit textual descriptions and
 412 implicit visual patterns.

412 Our framework initiates the ontology enrichment process with an initial 4D printing ontology, which
 413 comprises only 170 classes, 9 instances, 48 object properties, and 13 data properties. Through the
 414 successive integration of heterogeneous data sources and advanced validation techniques, the frame-
 415 work has dramatically enriched and populated the ontology. In the first phase, the system processed a
 416 corpus of scientific articles by extracting triplets that describe various domain-specific relationships.
 417 In total, approximately 130,000 triplets were initially generated from articles, of which only about
 418 28,000 were retained after applying the full consistency filtering pipeline, including semantic sim-
 419 ilarity checks, predicate template matching, and redundancy elimination. This stage resulted in the
 420 identification of 5,706 classes, 16,651 instances, 1,331 object properties, 4,390 data properties, and
 421 the establishment of 7,913 subclass relationships. The consideration of MatKG further augmented
 422 the ontology by processing additional instance-of relationships. It was responsible for incorporating
 423 6,629 new instances and two additional data properties with 445,370 relations. This considerable
 424 increase reflects the framework’s ability to integrate detailed instance-level data from supplementary
 425 sources, thereby enhancing the granularity and applicability of the ontology. A further enrichment
 426 occurred through the automated ingestion of multiple datasets from an external directory. This step
 427 contributed 144 additional classes, 12,540,671 instances, 26 object properties, and 113 subclass
 428 relationships (see **Figure 5**). By parsing and merging these large-scale datasets, the framework en-
 429 sured a comprehensive and diverse coverage of the domain knowledge, while maintaining structural
 430 validity and eliminating redundancy.

431 After synthesizing the contributions from the scientific literature, the MatKG module, and addi-
 432 tional datasets, the final ontology exhibits 5,849 classes, 12,563,951 instances, 1,357 object prop-
 433 erties, 4,392 data properties, and 8,196 subclass relationships. This substantial ontology expansion

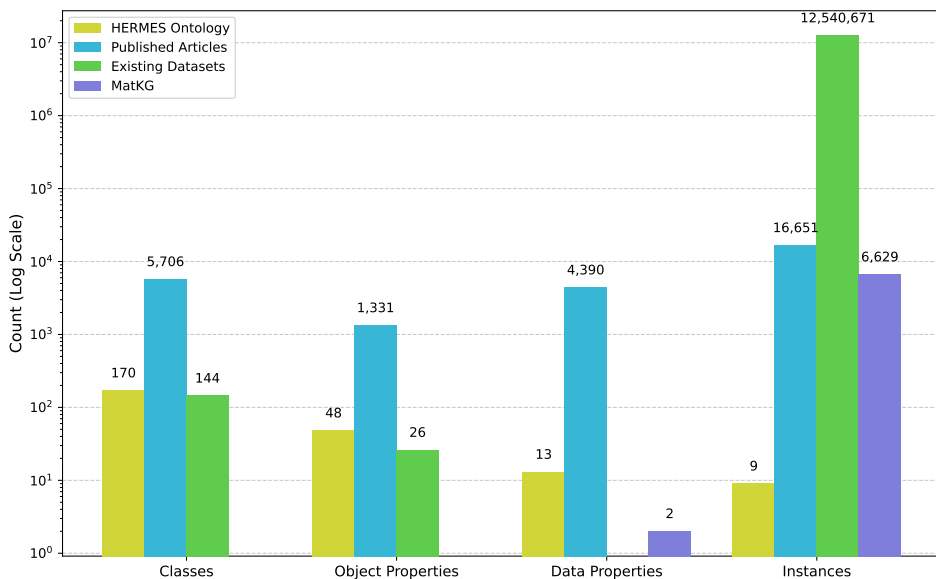


Figure 5: Comparison of ontology components between the baseline HERMES ontology and its extended counterparts derived from published articles processing, dataset parsing, and integration with MatKG triplet (adapted from (Bougzime et al., 2025b)).

demonstrates the efficacy of our multi-stage enrichment process, as illustrated in Appendix D, which highlights a subgraph centered on the stimuli-sensitive Hydrogel class.

In summary, the integration of multiple data sources, coupled with advanced NLP and robust validation measures, has culminated in a high-fidelity, richly structured ontology. Although our experimental validation focuses on 4D printing, this domain is inherently cross-disciplinary, spanning materials science, chemistry, additive manufacturing, process engineering, and smart structures. This framework is entirely domain-agnostic: adapting it to a new field would primarily involve changing the input corpus and the target ontology, while leaving the core retrieval, extraction, and validation pipeline unchanged. The resulting ontology not only represents a substantial expansion in scale and detail compared to its initial state but also provides a solid foundation for downstream applications such as knowledge-based reasoning, data integration, and semantic information retrieval across complex scientific and technical domains. When embedded within a neuro-symbolic AI (NSAI) framework, the ontology can be dynamically updated in real-time and reasoned over alongside neural models, thereby bridging symbolic and neural approaches for a context-aware design strategy (Bougzime et al., 2025a).

4 QUERY-ANSWER EXAMPLES FOR SMART MATERIALS AND STRUCTURES

The enriched ontology enables the formulation and resolution of design-oriented queries in 4D printing. To demonstrate its relevance, we encoded a material selection need as a semantic query vector in the ontology embedding space and retrieved the most relevant materials, experiments, and architectures by ranking their embeddings using cosine similarity. In this illustrative case, the design intent was: “Identify a soft, biocompatible material that is chemically compatible with LCE and printable via direct ink writing (DIW)”.

The highest-ranked neighborhood returned by cosine similarity was dominated by silicone-based elastomers. This ranking was supported by convergent evidence from the literature, including DIW-processable silicones such as polydimethylsiloxane (PDMS) formulations.

486 As the top-ranked result, the ontology retrieved PDMS as a soft silicone elastomer that can be pro-
 487 cessed by DIW using embedded/freeform strategies, where uncured PDMS inks were extruded into
 488 a hydrophilic support bath and subsequently cured into stable 3D features (Hinton et al., 2015; Li
 489 & Li, 2022). PDMS is also widely documented as biocompatible and chemically inert, which ex-
 490 plains its routine use in soft implantable systems (McDonald & Whitesides, 2002). Crucially for
 491 LCE compatibility, PDMS has been used as the passive silicone layer in bilayer systems integrating
 492 cholesteric or nematic LCE actuators, demonstrating that silicone-LCE interfaces can be formed and
 493 operated without reported interfacial chemical inhibition. Jiang et al. (2024); Li et al. (2024) Repre-
 494 sentative extracted triples include [PDMS, isPrintedUsing, DIW], [PDMS, is, Biocompatible], and
 495 [LCE actuator, isIntegratedWith, PDMS layer], confirming PDMS as a DIW-printable, biocompati-
 496 ble material compatible with LCE systems.
 497

498 We then evaluated a second design need: “Determine the material distribution of LCE and PDMS to
 499 ensure actuation and biocompatibility of the structure”. The ontology returned an embedded com-
 500 posite architecture, in which discrete LCE particles are dispersed within a continuous PDMS elas-
 501 tomer matrix. This configuration corresponds to reported polymer-dispersed LCE composites, where
 502 LCE particles provide localized anisotropic actuation and the PDMS matrix serves as a compliant
 503 host that transmits deformation while avoiding mechanical clamping of the LCE domains. Repre-
 504 sentative triples supporting this match include [LCE particles, isDispersedIn, PDMS matrix], [LCE
 505 composite, exhibits, Reversible actuation], and [PDMS, is, Biocompatible], all grounded in reported
 506 studies on LCE-PDMS composites and PDMS-based biomedical systems (Bobnar et al., 2023; Mc-
 507 Donald & Whitesides, 2002).

508 The enriched ontology demonstrated strong potential as a design-support system for 4D printing by
 509 enabling high-level, intent-driven queries to be translated into relevant recommendations. By em-
 510 bedding design intents into a semantic vector space and retrieving knowledge via similarity ranking,
 511 the ontology accurately identified DIW-printable, biocompatible silicone elastomers – particularly
 512 PDMS – as optimal matches for a active, LCE-compatible material, with results supported by litera-
 513 ture-derived triples and experimental reports. It further inferred an appropriate LCE-PDMS compos-
 514 ite architecture, retrieving evidence for embedded LCE domains within a compliant PDMS matrix
 515 that preserves actuation while ensuring biocompatibility. These examples illustrate the ontology’s
 516 ability to integrate heterogeneous knowledge, infer mechanistically coherent solutions, and guide
 517 material and structural design decisions, highlighting its promise as a generalizable and evidence-
 518 backed tool for accelerating discovery in smart material systems.
 519

520

521

522 5 CONCLUSION

523

524 In this work, we presented an innovative framework for ontology enrichment applicable across di-
 525 verse domains, integrating MLLMs and RAG to overcome the limitations of traditional ontological
 526 systems. Our approach, successfully combines the formal rigor of structured knowledge repre-
 527 sentation with the adaptive and contextual capabilities of advanced language models, which sys-
 528 tematically captures heterogeneous information from scientific literature, databases and extensive
 529 knowledge graphs. Experimental results demonstrate that our methodology significantly expanded
 530 an initial, rather limited ontology – starting from 170 classes and a few instances – to a compre-
 531 hensive structure encompassing over 5,800 classes and more than 12.5 million instances. Future
 532 work should focus on (i) designing specialized agent architectures that integrate vision encoders and
 533 domain-specific prompt templates for materials science modalities (Bougzime et al., 2025c;d), (ii)
 534 implementing advanced verification heuristics that leverage both linguistic and visual ontological
 535 rules, (iii) developing evaluation metrics for multimodal triplet extraction that reflect the unique
 536 challenges of materials knowledge representation, and (iv) creating dedicated relation classification
 537 agents for precise typing along with specialized validation agents for ontology cohesion and triplet
 538 integrity. By embracing multimodal multi-agent systems, we can move toward adaptive ontologies
 539 that evolve seamlessly with the scientific literature, providing researchers with powerful tools for
 accelerated materials discovery and development.

540 REFERENCES
541

542 Hydrogel design tools, 2023. URL <https://hydrogeldesign.org/tools/>.

543 Researchrabbit. <https://www.researchrabbit.ai/>, 2025.

544 Robert Arp, Barry Smith, and Andrew D. Spear. *Building Ontologies with Basic Formal Ontology*.
545 The MIT Press, 2015. ISBN 9780262527811.

546 Aspose. Aspose.PDF for Python via .NET. <https://pypi.org/project/aspose-pdf/>,
547 2024.

548 Matej Bobnar, Nikita Derets, Saide Umerova, Valentina Domenici, Nikola Novak, Marta Lavrič,
549 George Cordoyiannis, Boštjan Zalar, and Andraž Rešetič. Polymer-dispersed liquid crystal elas-
550 tomers as moldable shape-programmable materials. *Nature Communications*, 14:764, 2023. doi:
551 10.1038/s41467-023-36426-y.

552 Olivier Bodenreider. The unified medical language system (umls): integrating biomedical terminol-
553 ogy. *Nucleic Acids Research*, 32(suppl_1):D267–D270, 2004.

554 Oualid Bougzime, Christophe Cruz, Jean-Claude André, Kun Zhou, H Jerry Qi, and Frédéric De-
555 moly. Neuro-symbolic artificial intelligence in accelerated design for 4d printing: Status, chal-
556 lenges, and perspectives. *Materials & Design*, pp. 113737, 2025a. doi: 10.1016/j.matdes.2025.
557 113737.

558 Oualid Bougzime, Christophe Cruz, Kun Zhou, H. Jerry Qi, and Frédéric Demoly. Structuring
559 scientific knowledge for smart materials and 4d printing: An ontology enrichment framework
560 using retrieval-augmented large language models. *Computers in Industry*, 2025b. Under review.

561 Oualid Bougzime, Samir JABBAR, Christophe Cruz, and Frédéric DEMOLY. Evaluating neuro-
562 symbolic AI architectures: Design principles, qualitative benchmark, comparative analysis and
563 results. In *19th International Conference on Neurosymbolic Learning and Reasoning*, 2025c.
564 URL <https://openreview.net/forum?id=yCwcRijfxz>.

565 Oualid Bougzime, Samir Jabbar, Christophe Cruz, and Frédéric Demoly. Unlocking the potential
566 of generative ai through neuro-symbolic architectures–benefits and limitations. *arXiv preprint*
567 *arXiv:2502.11269*, 2025d.

568 Tom B. Brown, Benjamin Mann, Nick Ryder, Melanie Subbiah, Jared Kaplan, Prafulla Dhariwal,
569 Arvind Neelakantan, Pranav Shyam, Girish Sastry, Amanda Askell, et al. Language models are
570 few-shot learners. In *Advances in Neural Information Processing Systems*, volume 33, pp. 1877–
571 1901, 2020.

572 Nawaz Chungoora, Robert I. M. Young, G. Gunendran, C. Palmer, Z. Usman, and Keith Case.
573 Towards a formal ontology for product-service systems. *Computers in Industry*, 64(4):301–309,
574 2013.

575 John H Crews, Ralph C Smith, Kyle M Pender, Jennifer C Hannen, and Gregory D Buckner. Data-
576 driven techniques to estimate parameters in the homogenized energy model for shape memory
577 alloys. *Journal of Intelligent Material Systems and Structures*, 23(17):1897–1920, 2012.

578 Frédéric Demoly and Jean-Claude André. Is order creation through disorder in additive manufactur-
579 ing possible? *Cogent Engineering*, 8(1):1889110, 2021. doi: 10.1080/23311916.2021.1889110.

580 Frédéric Demoly and Jean-Claude André. *4D Printing, Volume 1: Between Disruptive Research*
581 *and Industrial Applications*. John Wiley & Sons, 2022a.

582 Frédéric Demoly and Jean-Claude André. *4D Printing, Volume 2: Between Science and Technology*.
583 John Wiley & Sons, 2022b.

584 Frédéric Demoly and Jean-Claude André. 4d printing: Bridging the gap between fundamen-
585 tal research and real-world applications. *Applied Sciences*, 14(13):5669, 2024. doi: 10.3390/
586 app14135669.

594 Frédéric Demoly, Martin L Dunn, Kristin L Wood, H Jerry Qi, and Jean-Claude André. The status,
 595 barriers, challenges, and future in design for 4d printing. *Materials & Design*, 212:110193, 2021.
 596

597 Frédéric Demoly and Jean-Claude André. Research strategy in 4d printing: Disruptive vs in-
 598 cremental? *Journal of Integrated Design and Process Science*, 24(2):53–73, 2021. doi:
 599 10.3233/JID200020.

600 Saoussen Dimassi, Frédéric Demoly, Christophe Cruz, H Jerry Qi, Kyoung-Yun Kim, Jean-Claude
 601 André, and Samuel Gomes. An ontology-based framework to formalize and represent 4d printing
 602 knowledge in design. *Computers in Industry*, 126:103374, 2021.

603 Dimitrios Doumanas, Andreas Souliaridis, Dimitris Spiliotopoulos, Costas Vassilakis, and Konstanti-
 604 nos Kotis. Fine-tuning large language models for ontology engineering: A comparative analysis
 605 of gpt-4 and mistral. *Applied Sciences*, 15(4):2146, 2025.

606 Yunfan Gao, Yun Xiong, Xinyu Gao, Kangxiang Jia, Jinliu Pan, Yuxi Bi, Yi Dai, Jiawei Sun, and
 607 Haofen Wang. Retrieval-augmented generation for large language models: A survey. *arXiv*
 608 preprint [arXiv:2312.10997](https://arxiv.org/abs/2312.10997), 2023.

609

610 Qi Ge, H Jerry Qi, and Martin L Dunn. Active materials by four-dimension printing. *Applied
 611 Physics Letters*, 103(13), 2013.

612

613 Hussam Ghanem and Christophe Cruz. Fine-tuning vs. prompting: evaluating the knowledge graph
 614 construction with llms. In *3rd International Workshop on Knowledge Graph Generation from
 615 Text (Text2KG) Co-located with the Extended Semantic Web Conference (ESWC 2024)*, volume
 616 3747, pp. 7, 2024.

617 Emanuele Ghedini, A Hashibon, J Friis, G Goldbeck, G Schmitz, and A De Baas. Emro the
 618 european materials modelling ontology. In *EMMC Workshop on Interoperability in Materials
 619 Modelling*, pp. 7–8. St John’s Innovation Centre Cambridge, 2017.

620

621 Thomas R. Gruber. A translation approach to portable ontology specifications. *Knowledge Acquisi-
 622 tion*, 5(2):199–220, 1993.

623

624 Nicola Guarino, Daniel Oberle, and Steffen Staab. What is an ontology? In *Handbook on Ontolo-
 625 gies*, pp. 1–17. Springer, 2009.

626

627 Timothy J. Hinton, Quentin Jallerat, Ryan N. Palchesko, Ji Won Park, Mark S. Grodzicki, Han-
 628 Jui Shue, Mohannad H. Ramadan, Adam R. Hudson, and Adam W. Feinberg. 3d printing pdms
 629 elastomer in a hydrophilic support bath via freeform reversible embedding. *Science Advances*, 1
 630 (9):e1500758, 2015. doi: 10.1126/sciadv.1500758.

631

632 Jordan Hoffmann, Sebastian Borgeaud, Arthur Mensch, Elena Buchatskaya, Trevor Cai, Eliza
 633 Rutherford, Diego de Las Casas, Lisa Anne Hendricks, Johannes Welbl, Aidan Clark, et al.
 634 Training compute-optimal large language models. In *Advances in Neural Information Processing
 635 Systems*, volume 35, 2022.

636

637 Anubhav Jain, Shyue Ping Ong, Geoffroy Hautier, Wei Chen, William Davidson Richards, Stephen
 638 Dacek, Shreyas Cholia, Dan Gunter, David Skinner, Gerbrand Ceder, et al. Commentary: The ma-
 639 terials project: A materials genome approach to accelerating materials innovation. *APL materials*,
 640 1(1), 2013a.

641

642 Anubhav Jain, Shyue Ping Ong, Geoffroy Hautier, Wei Chen, William Davidson Richards, Stephen
 643 Dacek, Shreyas Cholia, Dan Gunter, David Skinner, Gerbrand Ceder, et al. The materials project:
 644 A materials genome approach to accelerating materials innovation, 2013b.

645

646 Cheonsu Jeong. Domain-specialized llm: Financial fine-tuning and utilization method using mistral
 647 7b. *Journal of Intelligence and Information Systems*, 30(1):93–120, March 2024. ISSN 2288-
 648 4882. doi: 10.13088/jiis.2024.30.1.093. URL [http://dx.doi.org/10.13088/jiis.
 649 2024.30.1.093](http://dx.doi.org/10.13088/jiis.2024.30.1.093).

650

651 Albert Q Jiang, Alexandre Sablayrolles, Arthur Mensch, Chris Bamford, Devendra Singh Chaplot,
 652 Diego de las Casas, Florian Bressand, Gianna Lengyel, Guillaume Lample, Lucile Saulnier, et al.
 653 Mistral 7b. *arXiv preprint arXiv:2310.06825*, 2023.

648 Zhi-Chao Jiang, Qing Liu, Yao-Yu Xiao, and Yue Zhao. Liquid crystal elastomers for actuation:
 649 A perspective on structure-property-function relation. *Progress in Polymer Science*, 153:101829,
 650 2024. ISSN 0079-6700. doi: <https://doi.org/10.1016/j.progpolymsci.2024.101829>.

651

652 Daniel Jurafsky and James H. Martin. *Speech and Language Processing (3rd ed. draft)*. 2025. URL
 653 <https://web.stanford.edu/~jurafsky/slp3/>.

654

655 Seungone Kim, Se June Joo, Doyoung Kim, Joel Jang, Seonghyeon Ye, Jamin Shin, and Minjoon
 656 Seo. The cot collection: Improving zero-shot and few-shot learning of language models via
 657 chain-of-thought fine-tuning. *arXiv preprint arXiv:2305.14045*, 2023.

658

659 Christopher Kuenneth and Rampi Ramprasad. polyone data set – 100 million hypothetical polymers
 660 including 29 properties, 2022. URL <https://doi.org/10.5281/zenodo.7124188>.

661

662 Hang Li. Deep learning for natural language processing: advantages and challenges. *National
 663 Science Review*, 5(1):24–26, 2018.

664

665 Mingzhe Li, Farzad Gholami, Liang Yue, Marcus R Fratarcangeli, Elias Black, Shinnosuke
 666 Shimokawa, Tsuyoshi Nomura, Masato Tanaka, Hiroki Kobayashi, Yuyang Song, et al. Coaxial-
 667 spun hollow liquid crystal elastomer fiber as a versatile platform for functional composites. *Ad-
 668 vanced Functional Materials*, 34(42):2406847, 2024.

669

670 Yun Li and Bo Li. Direct ink writing 3d printing of polydimethylsiloxane-based soft and composite
 671 materials: a mini review. *Oxford Open Materials Science*, 2(1):itac008, 10 2022. doi: 10.1093/
 672 oxfmat/itac008.

673

674 Yunshui Li, Binyuan Hui, Xiaobo Xia, Jiaxi Yang, Min Yang, Lei Zhang, Shuzheng Si, Junhao
 675 Liu, Tongliang Liu, Fei Huang, et al. One shot learning as instruction data prospector for large
 676 language models. *arXiv preprint arXiv:2312.10302*, 2023.

677

678 Vladislav Lialin, Vijeta Deshpande, and Anna Rumshisky. Scaling down to scale up: A guide to
 679 parameter-efficient fine-tuning. *arXiv preprint arXiv:2303.15647*, 2023.

680

681 Chin-Yew Lin. Rouge: A package for automatic evaluation of summaries. In *Text summarization
 682 branches out*, pp. 74–81, 2004.

683

684 Haokun Liu, Derek Tam, Mohammed Muqeeth, Jay Mohta, Tenghao Huang, Mohit Bansal, and
 685 Colin A Raffel. Few-shot parameter-efficient fine-tuning is better and cheaper than in-context
 686 learning. *Advances in Neural Information Processing Systems*, 35:1950–1965, 2022.

687

688 John C. McDonald and George M. Whitesides. Poly(dimethylsiloxane) as a material for fab-
 689 ricing microfluidic devices. *Accounts of Chemical Research*, 35(7):491–499, 2002. doi:
 690 10.1021/ar010110q.

691

692 Jacob Murel and Joshua Noble. What is llm temperature? <https://www.ibm.com/think/topics/llm-temperature>, 2024.

693

694 NASA. Nasa shape memory repository. <https://shapememory.grc.nasa.gov/>, 2025.

695

696 Nlm-atics. Llmsherpa: Developer apis to accelerate llm projects. <https://github.com/nlmatics/llmsherpa>, 2024. GitHub repository.

697

698 Kishore Papineni, Salim Roukos, Todd Ward, and Wei-Jing Zhu. Bleu: a method for automatic
 699 evaluation of machine translation. In *Proceedings of the 40th annual meeting of the Association
 700 for Computational Linguistics*, pp. 311–318, 2002.

701

Venkatesh Balavadhani Parthasarathy, Ahtsham Zafar, Aafaq Khan, and Arsalan Shahid. The ul-
 702 timate guide to fine-tuning llms from basics to breakthroughs: An exhaustive review of tech-
 703 nologies, research, best practices, applied research challenges and opportunities. *arXiv preprint
 704 arXiv:2408.13296*, 2024.

Baolin Peng, Chunyuan Li, Pengcheng He, Michel Galley, and Jianfeng Gao. Instruction tuning
 705 with gpt-4. *arXiv preprint arXiv:2304.03277*, 2023.

702 Xirui Peng, Shuai Wu, Xiaohao Sun, Liang Yue, S Macrae Montgomery, Frédéric Demoly, Kun
 703 Zhou, Ruike Renee Zhao, and H Jerry Qi. 4d printing of freestanding liquid crystal elastomers
 704 via hybrid additive manufacturing. *Advanced Materials*, 34(39):2204890, 2022.

705 Mina Abd Nikooie Pour, Huanyu Li, Rickard Armiento, and Patrick Lambrix. Phrase2onto: A tool
 706 to support ontology extension. *Procedia Computer Science*, 225:1415–1424, 2023.

708 Nathan R Richbourg and Nicholas A Peppas. Structurally decoupled stiffness and solute transport
 709 in multi-arm poly (ethylene glycol) hydrogels. *Biomaterials*, 301:122272, 2023.

710 NR Richbourg, M Wancura, AE Gilchrist, S Toubbeh, BAC Harley, E Cosgriff-Hernandez, and
 711 NA Peppas. Precise control of synthetic hydrogel network structure via linear, independent
 712 synthesis-swelling relationships. *Science Advances*, 7(7):eabe3245, 2021.

714 Swarnadeep Saha, Prateek Yadav, Lisa Bauer, and Mohit Bansal. Explagraphs: An explanation
 715 graph generation task for structured commonsense reasoning. *arXiv preprint arXiv:2104.07644*,
 716 2021.

717 Nigel Shadbolt, Tim Berners-Lee, and Wendy Hall. The semantic web revisited. *IEEE Intelligent
 718 Systems*, 21(3):96–101, 2006.

720 Barry Smith. Mereotopology: A theory of parts and boundaries. *Data & Knowledge Engineering*,
 721 20(3):287–303, 1996. doi: [https://doi.org/10.1016/S0169-023X\(96\)00015-8](https://doi.org/10.1016/S0169-023X(96)00015-8).

723 Kei-ichiro Takahashi, Hiroshi Mamitsuka, Masatoshi Tosaka, Nanyi Zhu, and Shigeru Yamago.
 724 Copoldb: a copolymerization database for radical polymerization. *Polymer Chemistry*, 15(10):
 725 965–971, 2024.

726 Skylar Tibbits. The emergence of “4d printing”. In *TED conference*, 2013.

728 Talip Ucar, Adrian Gonzalez-Martin, Matthew Lee, and Adrian Daniel Szwarc. One-shot learning
 729 for language modelling. *arXiv preprint arXiv:2007.09679*, 2020.

730 University of Chicago. Polymer property predictor and database (pppdb), 2023. URL <https://pppdb.uchicago.edu/>.

733 Mikel Val-Calvo, Mikel Egaña Aranguren, Juan Mulero-Hernández, Ginés Almagro-Hernández,
 734 Prashant Deshmukh, José Antonio Bernabé-Díaz, Paola Espinoza-Arias, José Luis Sánchez-
 735 Fernández, Juergen Mueller, and Jesualdo Tomás Fernández-Breis. Ontogenix: Leveraging large
 736 language models for enhanced ontology engineering from datasets. *Information Processing &
 737 Management*, 62(3):104042, 2025.

738 Vineeth Venugopal and Elsa Olivetti. Matkg: An autonomously generated knowledge graph in
 739 material science. *Scientific Data*, 11(1):217, 2024.

740 Jason Wei, Xuezhi Wang, Dale Schuurmans, Maarten Bosma, Fei Xia, Ed Chi, Quoc V Le, Denny
 741 Zhou, et al. Chain-of-thought prompting elicits reasoning in large language models. *Advances in
 742 neural information processing systems*, 35:24824–24837, 2022.

744 Guanchen Wu, Chen Ling, Ilana Graetz, and Liang Zhao. Ontology extension by online clustering
 745 with large language model agents. *Frontiers in Big Data*, 7:1463543, 2024.

747 Zhengyuan Yang, Zhe Gan, Jianfeng Wang, Xiaowei Hu, Yumao Lu, Zicheng Liu, and Lijuan Wang.
 748 An empirical study of gpt-3 for few-shot knowledge-based vqa. In *Proceedings of the AAAI
 749 conference on artificial intelligence*, volume 36, pp. 3081–3089, 2022.

750 Shukang Yin, Chaoyou Fu, Sirui Zhao, Ke Li, Xing Sun, Tong Xu, and Enhong Chen. A survey
 751 on multimodal large language models. *National Science Review*, 11(12):nwae403, 11 2024. doi:
 752 10.1093/nsr/nwae403.

753 Yujia Zhang, Tyler Sadler, Mohammad Reza Taesiri, Wenjie Xu, and Marek Reformat. Fine-tuning
 754 language models for triple extraction with data augmentation. In *Proceedings of the 1st Workshop
 755 on Knowledge Graphs and Large Language Models (KaLLM 2024)*, pp. 116–124, 2024.

756 A AI MODEL ASSESSMENT
757
758
759

760 To determine the optimal temperature – a key parameter that regulates the level of randomness
761 in the model’s output during inference – we evaluated the model’s performance across a range of
762 temperature settings. Specifically, we tested two configurations: the fine-tuned model on its own,
763 and the fine-tuned model combined with one-shot learning. Temperature plays an important role
764 in balancing determinism and creativity in language model outputs. Lower temperatures make the
765 model’s responses more focused and predictable, while higher temperatures increase variability and
766 originality. This trade-off impacts the accuracy and relevance of extracted triplets (Murel & No-
767 bable, 2024). As illustrated in **Figure 6**, the standard fine-tuning approach without any in-context
768 learning demonstrated higher stability and improved performance when compared to the fine-tuning
769 approach with one-shot across metrics which represent n-gram-based metrics encompassing preci-
770 sion (Bilingual Evaluation Understudy, termed as BLEU), Recall-Oriented Understudy for Gisting
771 Evaluation (termed as ROUGE), and F1-score (combining BLEU and ROUGE metrics) (Ghanem
772 & Cruz, 2024). These n-gram-based metrics rely on the comparison of overlapping word sequences
773 (called n-grams) between the generated and reference texts. For instance, an e -gram refers to a con-
774 tinuous sequence of e words, 1-grams are unigrams (single words), 2-grams are bigrams, and so on,
775 thus providing nuanced evaluation of fluency and relevance in generated text (Jurafsky & Martin,
776 2025). Details of the metric computation are provided in the next section.

776 In addition to large-scale quantitative enrichment, we performed a qualitative assessment by man-
777 ually reviewing a representative subset of extracted triples (top-k highest confidence predictions and
778 a random sample of 200 instances) compared to expert knowledge. The evaluation considered four
779 dimensions: (i) relevance of the extracted relation to the 4D printing domain, (ii) factual correct-
780 ness with respect to the source text, (iii) clarity of entity boundaries and relation semantics, and
781 (iv) actionability in terms of whether the triple can be meaningfully integrated into downstream
782 ontology reasoning. For instance, the extracted triple [Hydrogel, isInstanceOf, Biocompat-
783 ible_Material] was judged as fully correct and relevant, whereas [3D_printing, converts, Ro-
784 bust_manufacturing_process], although syntactically valid, was marked as semantically unclear
785 and thus of limited actionability. Overall, 84% of the reviewed triples were rated as both factually
786 correct and relevant, 10% as partially correct but ambiguous (e.g., inconsistent entity typing), and 6%
787 as incorrect due to model hallucinations or misalignment. This analysis highlights that while large-
788 scale automatic enrichment can produce “shallow” or noisy entries, systematic sampling and expert
789 review confirm that the majority of extracted triples are suitable for ontology integration. Qualita-
790 tively, these proportions indicate that high-confidence extractions are immediately usable, whereas
791 most residual errors stem from entity typing and boundary delineation; this highlights schema-aware
792 normalization and predicate templating as the primary levers for improvement. Error forensics fur-
793 ther show that low-evidence contexts and predicate drift account for the majority of the remaining
794 6% failures, motivating a quarantine queue and tighter domain/range constraints prior to graph in-
795 sertion. Taken together, these observations align with our objectives—precision under ontological con-
796 straints and provenance-backed integration—and directly inform corrective actions in the pipeline
797 (stricter typing, evidence thresholds, and conflict-aware deduplication). Beyond this qualitative view,
798 we performed a quantitative analysis showing that the stand-alone fine-tuned model consistently out-
799 performs the fine-tuned-plus-one-shot configuration, which exhibits pronounced variability and uni-
800 formly lower scores. Triplet-matching F1 peaks at $T \approx 0.55$, while G-BLEU and G-ROUGE remain
801 optimal over $T \in [0.55, 0.70]$; G-BERTScore precision is maximal near $T \approx 0.55$, indicating fine-
802 grained semantic alignment between predicted and reference graphs. Taken together, these results
803 show that $T \approx 0.55$ offers the best precision-recall trade-off, combining robust F1 with sensitivity
804 captured by both n-gram overlap and contextualized embeddings. Consequently, plain fine-tuning
805 delivers superior extractive accuracy and stability for relational triple extraction while avoiding the
806 complexity and instability introduced by one-shot in-context learning. Analytically, this justifies fix-
807 ing $T = 0.55$ as the default decoding regime to prioritize precision without collapsing recall; opera-
808 tionally, it implies fewer low-confidence triples entering pre-insertion quarantine and, downstream,
809 fewer ontology-coherence violations – i.e., a larger yet cleaner graph.

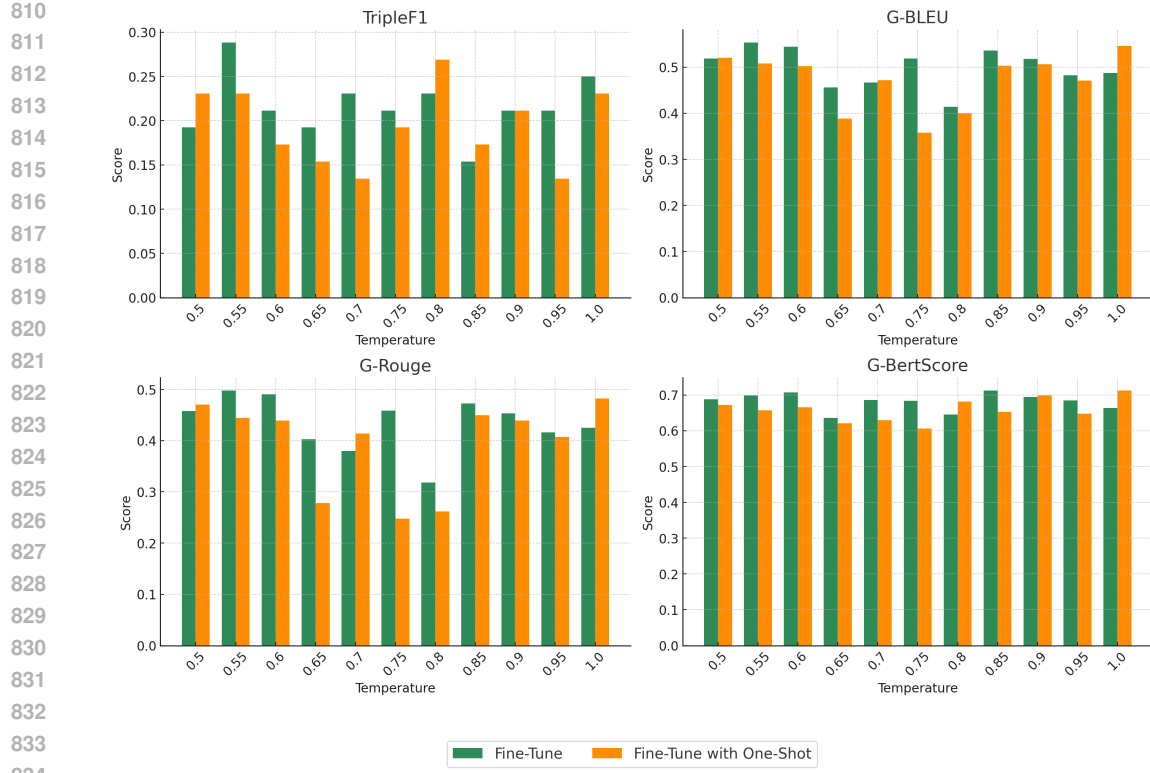


Figure 6: Comparison metrics between prompt with the fine-tuned model vs. prompt with the fine-tuned model using one-shot technique performance across various temperatures (adapted from (Bougzime et al., 2025b)).

B METRIC COMPUTATION

BLEU-F1 Score (Papineni et al., 2002)

Let C_{gen} be the number of 4-grams in the generated graph, C_{ref} the number of 4-grams in the reference graph, and C_{match} the number of matching 4-grams. Then:

$$P_{\text{Bleu}} = \frac{C_{\text{match}}}{C_{\text{gen}}} \quad (1)$$

$$R_{\text{Bleu}} = \frac{C_{\text{match}}}{C_{\text{ref}}} \quad (2)$$

$$F1^{\text{Bleu}} = \frac{2 P_{\text{Bleu}} R_{\text{Bleu}}}{P_{\text{Bleu}} + R_{\text{Bleu}}} \quad (3)$$

ROUGE-F1 Score (Lin, 2004)

For ROUGE-2 (bigrams), let $\text{bigram}_{\text{cand}}$ and $\text{bigram}_{\text{ref}}$ be the sets of bigrams in the candidate and reference, respectively. Then

$$P_{\text{ROUGE}} = \frac{|\text{bigram}_{\text{cand}} \cap \text{bigram}_{\text{ref}}|}{|\text{bigram}_{\text{cand}}|} \quad (4)$$

$$R_{\text{ROUGE}} = \frac{|\text{bigram}_{\text{cand}} \cap \text{bigram}_{\text{ref}}|}{|\text{bigram}_{\text{ref}}|} \quad (5)$$

$$F1^{\text{ROUGE}} = \frac{2 P_{\text{ROUGE}} R_{\text{ROUGE}}}{P_{\text{ROUGE}} + R_{\text{ROUGE}}} \quad (6)$$

864 **Graph BERTScore (G-BS) (Saha et al., 2021)**

865 G-BS takes graphs as a set of edges and solves a matching problem which finds the best alignment
 866 between the edges in the predicted graph and those in the ground-truth graph. Each edge is
 867 considered as a “sentence” and BERTScore is used to calculate the similarity between a pair of pre-
 868 dicted and ground-truth edges. Based on the optimal alignment and the overall matching score, the
 869 computed F1 score is used as the final G-BERTScore.

870 Considering x_i as a reference token (entity or relation) and \hat{x}_j as a generated token (entity or relation),
 871 the complete score matches each token in x to a generated token in \hat{x} to compute recall, and
 872 each token in \hat{x} to a token in x to compute precision. A greedy matching was used to maximize the
 873 total similarity score, where each token was matched to the most similar token in the other graph.
 874 Then precision and recall were combined to compute an F1 measure.

875 For a reference sequence $x = \{x_1, \dots, x_{|x|}\}$ and a candidate sequence $\hat{x} = \{\hat{x}_1, \dots, \hat{x}_{|\hat{x}|}\}$, the
 876 recall R , precision P , and F1 scores are defined as:

$$878 \quad R_{\text{BERT}} = \frac{1}{|x|} \sum_{x_i \in x} \max_{\hat{x}_j \in \hat{x}} x_i^\top \hat{x}_j \quad (7)$$

$$881 \quad P_{\text{BERT}} = \frac{1}{|\hat{x}|} \sum_{\hat{x}_j \in \hat{x}} \max_{x_i \in x} x_i^\top \hat{x}_j \quad (8)$$

$$884 \quad F_1^{\text{BERT}} = \frac{2 P_{\text{BERT}} R_{\text{BERT}}}{P_{\text{BERT}} + R_{\text{BERT}}} \quad (9)$$

886 **Triples Matching (T-F1)**

887 The F1 score for triple matches T-F1 was calculated as follows:

$$888 \quad T\text{-}F1 = \frac{2 \text{TP}}{2 \text{TP} + \text{FP} + \text{FN}} \quad (10)$$

891 where TP is the number of true positive triple matches, FP is the number of false positive triple
 892 matches, and FN is the number of false negative triple matches. These metrics could potentially
 893 yield even better results if synonyms of entities or relations are considered as exact matches. This
 894 evaluation serves as a benchmark analysis for assessing the efficacy of our ontology enrichment
 895 methodology.

896

C EXPERIMENTAL SECTION

899 LLaVA was fine tuned using LoRA to improve triplet extraction. This technique allowed us to effi-
 900 ciently adjust the model’s parameters while minimizing resource consumption. The fine-tuning pro-
 901 cess utilized a synthetic dataset specifically designed to include textual and visual contexts aligned
 902 with the needs of 4D printing. In this process, LoRA was enabled with a rank of 128 and an alpha
 903 value of 256, and the multimodal projector learning rate was set to 2×10^{-5} . The base model used
 904 was liuhaojian/llava-v1.5-7b (version v1), and the training data comprised a synthetic
 905 dataset alongside an image folder containing the extracted images. The vision tower was configured
 906 to use OpenAI’s CLIP ViT-Large-Patch14-336, while the multimodal projector was set to an MLP
 907 with GELU activation (mlp2x_gelu), selecting the penultimate layer for vision features. Notably,
 908 both image start-end tokens and image patch tokens were disabled, and images were preprocessed
 909 with a padded aspect ratio. The training procedure grouped samples by modality length and lever-
 910 aged bfloat16 precision. Training was conducted for 5 epochs with a per-device batch size of 8 for
 911 training (and 4 for evaluation), accumulating gradients over 2 steps. The evaluation strategy was
 912 disabled during training, and model checkpoints were saved every 50,000 steps with a total check-
 913 point limit of one. The learning rate was fixed at 2×10^{-4} with no weight decay and a warmup ratio
 914 of 3%, using a cosine learning rate scheduler. Additionally, TF32 was enabled, the maximum model
 915 length was set to 2,048 tokens, gradient checkpointing was employed to conserve memory, and 4
 916 dataloader workers were used in conjunction with lazy preprocessing. **Figure 7** shows a rapid early
 917 loss drop followed by a low-variance plateau (~ 0.05), indicating stable convergence under LoRA
 918 (rank= 128, $\alpha = 256$) and supporting this fine-tuned LLaVA configuration as an appropriate and
 919 reliable model for triplet extraction.

All inferences were run on a single NVIDIA A40 GPU, with an average runtime of about one minute per prompt for the fine-tuned model, compared to approximately seven minutes per prompt for the few-shot configuration, highlighting a substantial gain in computational efficiency.



Figure 7: Training loss during LoRA fine-tuning of LLaVA for triplet extraction (reported by Weights & Biases).

D ONTOLOGY VIEW CENTERED ON THE HYDROGEL CLASS

This appendix provides a zoomed-in view of the final enriched ontology around the Hydrogel class. The graph illustrates how literature-derived triplets, dataset instances, and knowledge graph imports jointly populate stimuli-sensitive hydrogels and their related properties, processes, and functional roles (See **Figure 8**).

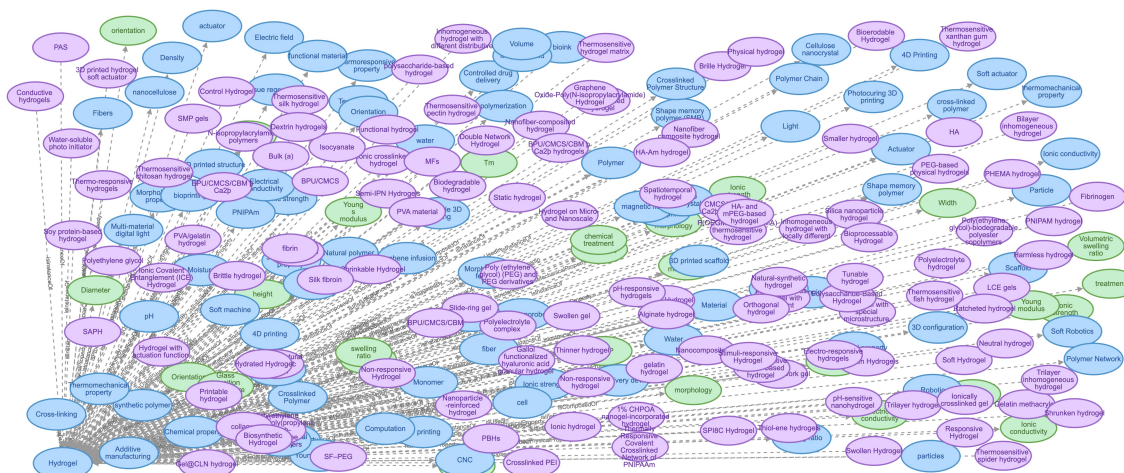


Figure 8: Final enriched 4D printing ontology through the lens of the stimuli-sensitive Hydrogel class. To ensure clarity, only a limited number of classes, object properties, and instances are displayed (adapted from (Bougzime et al., 2025b)).